



**HAL**  
open science

## Progressive melting in confined one-dimensional C 60 chains

Colin Bousige, Stéphan Rols, Erwan Paineau, Stéphan Rouzière, Cristian Mocuta, Bart Verberck, Jonathan P. Wright, Hiromichi Kataura, Pascale Launois, Stéphane Rols, et al.

► **To cite this version:**

Colin Bousige, Stéphan Rols, Erwan Paineau, Stéphan Rouzière, Cristian Mocuta, et al.. Progressive melting in confined one-dimensional C 60 chains. *Physical Review B: Condensed Matter and Materials Physics* (1998-2015), 2012, 86 (4), pp.45446 - 45446. 10.1103/PhysRevB.86.045446 . hal-01611946

**HAL Id: hal-01611946**

**<https://hal.science/hal-01611946>**

Submitted on 6 Oct 2017

**HAL** is a multi-disciplinary open access archive for the deposit and dissemination of scientific research documents, whether they are published or not. The documents may come from teaching and research institutions in France or abroad, or from public or private research centers.

L'archive ouverte pluridisciplinaire **HAL**, est destinée au dépôt et à la diffusion de documents scientifiques de niveau recherche, publiés ou non, émanant des établissements d'enseignement et de recherche français ou étrangers, des laboratoires publics ou privés.

**Progressive melting in confined one-dimensional C<sub>60</sub> chains**Colin Bousige,<sup>1,2</sup> Stéphane Rols,<sup>2,\*</sup> Erwan Paineau,<sup>1</sup> Stéphan Rouzière,<sup>1</sup> Cristian Mocuta,<sup>3</sup> Bart Verberck,<sup>4</sup> Jonathan P. Wright,<sup>5</sup> Hiromichi Kataura,<sup>6</sup> and Pascale Launois<sup>1,†</sup><sup>1</sup>Laboratoire de Physique des Solides, UMR CNRS 8502, Université Paris-Sud, F-91405 Orsay, France<sup>2</sup>Institut Laue Langevin, 6 rue Jules Horowitz, Boîte Postale 156, F-38042 Grenoble Cedex 9, France<sup>3</sup>Synchrotron SOLEIL, Saint-Aubin, Boîte Postale 48, 91192 Gif-sur-Yvette Cedex, France<sup>4</sup>Departement Fysica, Universiteit Antwerpen, Groenenborgerlaan 171, B-2020 Antwerpen, Belgium<sup>5</sup>European Synchrotron Radiation Facility, BP-220, F-38043 Grenoble Cedex 9, France<sup>6</sup>Nanosystem Research Institute, National Institute of Advanced Industrial Science and Technology, Central 4, Higashi 1-1-1, Tsukuba, Ibaraki 305-8562, Japan

(Received 29 February 2012; revised manuscript received 25 May 2012; published 26 July 2012)

C<sub>60</sub> fullerenes confined inside single-walled carbon nanotubes form an archetypal one-dimensional system. X-ray diffraction experiments, from room temperature to 1073 K, reveal an increasing melting phenomenon. Detailed analysis of the sawtooth peak characteristic of the fullerene organization allows the quantitative determination of fluctuations in intermolecular distances. The present results validate the predictions of one-dimensional statistical models.

DOI: [10.1103/PhysRevB.86.045446](https://doi.org/10.1103/PhysRevB.86.045446)

PACS number(s): 61.48.De, 61.46.Fg, 64.70.Nd, 61.05.cp

**I. INTRODUCTION**

One-dimensional (1D) systems are not only curiosities in nature, they are also of fundamental interest as they provide physicists with models that are analytically solvable. Despite their apparent simplicity, their ability to capture the essence of the physics at stake in more complex systems has given 1D systems a central role, and an extensive theoretical literature exists on the subject.<sup>1</sup> The realization of real 1D atomic or molecular arrangements in the 1970s and 1980s,<sup>2-4</sup> making it finally possible for an experimental study of theoretical models, has led to considerable attention toward physics in one dimension. This interest exceeds the domain of physics and extends to biological structures such as DNA.<sup>5,6</sup> However, none of the existing 1D systems was stable at high temperature. This is why the discovery of single-walled carbon nanotube (SWNT) inclusion compounds has once again highlighted 1D systems and their particular thermodynamics. A model 1D system is indeed obtained when C<sub>60</sub> fullerenes are encapsulated inside SWNTs with diameters close to 1.4 nm, resulting in the “peapods,”<sup>7</sup> this system showing an exceptional stability (up to ~1100 K before the fullerenes coalesce<sup>8</sup>). This stability led to an important theoretical activity, since peapods offered the possibility to study high-temperature 1D states experimentally. However, for 1D systems, diffraction measurements, which give access to their structural properties, are complicated by the extension of the response in reciprocal space, especially when single crystals are not available, as is the case for peapods. We present here a quantitative analysis of the structural and thermodynamical properties of C<sub>60</sub> fullerene chains for a powderlike sample. It should be of interest for further analyses of other 1D systems, of physical or biological relevance.

An elegant way of describing the evolution of the C<sub>60</sub> chains was provided by Girifalco and Hodak,<sup>9,10</sup> who applied classical tools in statistical 1D physics—such as the Takashi-Gürsey (TG) model—to this problem. This model, completed by Monte Carlo simulations,<sup>11,12</sup> allows predictions of the stable state as a function of temperature depending on the filling ratio of the tubes by fullerenes. The outcome of these studies

is that a progressive transformation of the chains occurs upon heating. This transformation involves both the fragmentation of the chains into smaller clusters, referred to as “clustering” in the following, and the progressive loss of periodicity inside one cluster due to thermal fluctuations. The clustering effect is dominant for small filling ratios, but is limited by the availability of voids inside the nanotubes. *At high density, no clustering is possible.* However, the thermal fluctuations are responsible for the strong increase of the liquidlike character of the chains with temperature, *even for complete filling.*<sup>10</sup> It is this progressive melting of the C<sub>60</sub> chains that caught our interest as, to the best of our knowledge and despite numerous theoretical studies, it had never been evidenced experimentally. We used x-ray diffraction (XRD) to investigate this transition because it is a nondestructive method allowing us to obtain statistical information from large (mm<sup>3</sup>) samples. We will show that the TG model provides a rather good description of the progressive melting occurring in C<sub>60</sub> peapods with high filling rate.

**II. THEORETICAL MODEL**

XRD measurements give access to the C<sub>60</sub> longitudinal pair correlation function  $G(z)$  in each SWNT, which, in the case of an infinite chain of molecules, can be written as follows:<sup>3</sup>

$$G(z) = \delta(z) + \sum_{m=1}^{\infty} [h_m(z) + h_m(-z)], \quad (1)$$

the distribution of the  $m$ th neighbor  $h_m(z)$  being given by the  $(m - 1)$  fold convolution product of the first-neighbor distribution function  $h(z)$ . This function was calculated by Girifalco and Hodak<sup>10</sup> using the TG model, in the limit of a very large number of molecules  $N$  in the system. Using their model and the intermolecular potential chosen in Refs. 9 and 10, we have calculated  $h(z)$  for various temperatures and SWNT filling ratios  $\tau$ . We performed a calculation of the pair correlation function, following the method detailed in Ref. 10, to obtain simulated diffraction diagrams for any filling rate

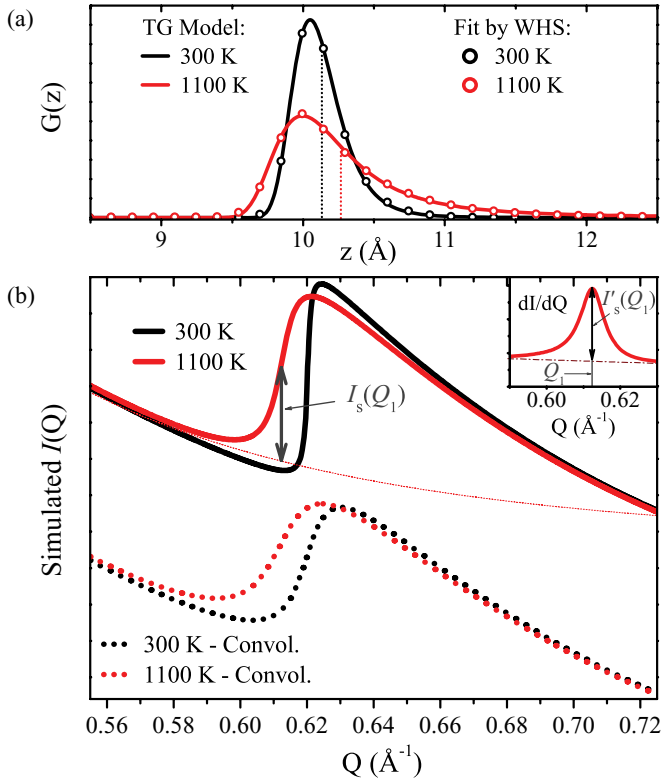


FIG. 1. (Color online) Temperature evolution of the correlation function and simulated diffraction diagrams. (a) First peak of the correlation function  $G(z)$  as obtained from the TG model at 300 and 1100 K for a 0.97 filling rate (full lines). The vertical dotted lines indicate the mean inter- $C_{60}$  distances  $\langle L \rangle$ , and the empty dots correspond to the fit of  $G(z)$  by a WHS model. (b) Simulated x-ray diffraction diagrams using the parameters from the WHS model (full lines). The inset shows the derivative of the simulated diffraction diagram at 1100 K. Dotted lines correspond to simulation after convolution of  $S(Q_z)$  by a resolution Lorentzian function with a FWHM of  $1 \times 10^{-2} \text{ \AA}^{-1}$ .

and temperature of interest for a detailed comparison with our experimental data. This allowed us to calculate parameters of interest with respect to experiment, such as, for instance, the  $\beta$  parameter, related to interfullerene correlations, discussed in the following. The resulting  $G(z)$  functions are shown in Fig. 1(a) for  $\tau = 0.97$  at 300 and 1100 K. We found that the form of these distribution functions can be reproduced by the weak hard spheres model (WHS) described by Rosshirt *et al.*<sup>3</sup> [empty dots in Fig. 1(a)], where the nearest-neighbor pair correlation function is expressed as the convolution product of that of a hard sphere liquid—with a shortest distance  $c$  and a characteristic width  $\sigma_1$ —with a Gaussian of width  $\sigma_2$ :

$$h(z) = \frac{1}{\sqrt{2\pi}\sigma_1\sigma_2} \int_c^\infty dt e^{-\frac{(t-z)^2}{2\sigma_2^2} - \frac{t-c}{\sigma_1}} \quad (2)$$

The mean intermolecular distance is calculated to be equal to

$$\langle L \rangle = c + \sigma_1 \quad (3)$$

while the root mean square deviation is found to be equal to  $\sqrt{\sigma_1^2 + \sigma_2^2}$ .

Following the calculations presented in Ref. 3, one finds that the structure factor  $S(Q_z)$ —the Fourier transform of the pair correlation function  $G(z)$ —of such an infinite chain is

$$S(Q_z) = \frac{1 - \rho^2}{1 + \rho^2 - 2\rho \cos(\theta)} + 2\pi\delta(\theta), \quad (4)$$

where  $\rho$  and  $\theta$  originate from the Fourier transform of  $h(z)$  expressed in the form  $H(Q_z) = \rho e^{i\theta}$ . For the WHS model,  $H(Q_z) = e^{-Q_z^2\sigma_2^2/2} e^{iQ_z c} / (1 - iQ_z\sigma_1)$ .

Equation (4) is the well known structure factor expression of a 1D liquid at finite temperature.<sup>2-4</sup> In infinite 1D systems, and in particular in the case of  $C_{60}$  chains,<sup>13</sup> the cumulative thermal fluctuations are expected to prevent the establishment of long-range order for any nonzero temperature. However, to the best of our knowledge, before the present study no experimental evidence was given for this liquidlike character; x-ray and electron diffraction data<sup>14,15</sup> were analyzed assuming that  $C_{60}$  molecules formed a 1D crystal, whose Bragg peaks are Dirac functions.

To simulate the intensity scattered by a powder of liquid  $C_{60}$  chains, one has to integrate  $S(Q_z)$  in Eq. (4) over all the possible orientations of the scattering vector  $\vec{Q}$ . Within the homogeneous approximation, the form factor of the  $C_{60}$  molecule can be written as  $F(Q) = 60 f_C(Q) \text{sinc}(Qr_{C_{60}})$ , where  $r_{C_{60}}$  is the molecule radius and  $f_C(Q)$  is the x-ray scattering factor of a carbon atom. The scattered intensity is then given by

$$I(Q) \propto F^2(Q) \int_{\xi=0}^1 S(Q\xi) d\xi \quad (5)$$

and is represented in Fig. 1(b) for infinite chains with the distribution functions in Fig. 1(a).

The simulated XRD diagrams present an asymmetric sawtooth peak characteristic of a powder of 1D chains.<sup>15,16</sup> The position of the inflection point  $Q_1$  on the left side of the peak is linked to the mean inter- $C_{60}$  distance by  $Q_1 = 2\pi/\langle L \rangle$ . We will introduce here the quantity  $\beta = \frac{I'_s(Q_1)}{I_s(Q_1)}$ ,  $I'_s(Q_1)$  being the slope of the sawtooth peak at  $Q_1$  and  $I_s(Q_1)$  its intensity [see Fig. 1(b) and its inset]. This  $\beta$  parameter is an indicator of the correlation length of the chains, since it is found to be proportional to  $(\sigma_1^2 + \sigma_2^2)^{-1}$ .<sup>22</sup> Therefore, any change in the thermodynamic state of the confined chains will result in a modification of the two parameters  $Q_1$  and  $\beta$ . The evolution of  $Q_1$  and  $\beta$ , respectively, linked to the average inter- $C_{60}$  distance and to the correlation length, is used to characterize the melting of the chains—loss of periodicity. A careful analysis of the experimental data and a comparison with the theoretical predictions will thus allow us to determine the thermodynamic state of the chains.

### III. EXPERIMENTAL

We have prepared  $C_{60}$  peapods samples in the form of buckypapers, according to Ref. 17. The samples were further pressed into pellets to increase their 2D anisotropy. The XRD measurements were performed on two different synchrotron beamlines: DIFFABS at synchrotron SOLEIL, using a Bühler oven under  $10^{-6}$  mbar vacuum, and ID11 at the ESRF, using a Linkam oven under 5 mbar  $N_2$ . The x rays' incoming

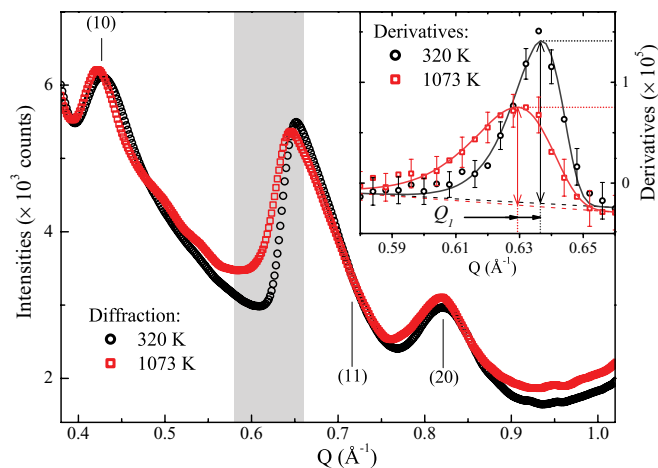


FIG. 2. (Color online) X-ray diffraction diagrams of peapods at 320 and 1073 K. Bundle peaks are indexed with  $(hk)$ . The rising step of the asymmetric peak characteristic of the 1D chains of  $C_{60}$  is highlighted in gray. The inset shows the evolution of the derivative of the diffraction diagram within the shaded area (symbols) and its fit (lines) by a Gumbel function  $(\frac{A}{B} e^{-b(z-C)/B} e^{-e^{-b(z-C)/B}})$  with  $b = 2.4464$  and a linear background (dashed lines). Its maximum position is  $Q_1$  and its maximum value gives the slope  $I'_s(Q_1)$ .

wavelengths were 1.409 and 0.3439 Å, respectively. The resolution was  $\simeq 1 \times 10^{-2} \text{ Å}^{-1}$  [full width at half-maximum (FWHM)] on both diffractometers. The results obtained with four different samples following the temperature ramp shown in the inset to Fig. 3(a) are reproducible and are discussed as one. The patterns were collected on area detectors, and azimuthal integrations were performed on angular sections ( $\sim 20^\circ$ ) where the signal from the chains was maximal. Typical XRD diagrams measured at room temperature and 1073 K are shown in Fig. 2. They contain the sawtooth peak at  $0.64 \text{ Å}^{-1}$ , characteristic of the 1D ordering of the fullerenes inside the tubes. In addition, the diagrams feature peaks characteristic of the organization of the peapods in hexagonal bundles, and indexed  $(hk)$  in the reciprocal hexagonal lattice. Detailed simulations of the diffraction diagrams following the method described in Ref. 15 show that the filling rate is 90%. We should stress that it is a mean filling rate over the whole sample, since empty tubes (badly opened) or portions of tubes, not accessible to fullerenes due to some defects, for instance, do contribute to its determination. The true filling rate inside well opened nanotubes is thus higher than 90%. Compared to the case of a powder, the 2D anisotropy allows maximization of the intensity of the sawtooth peak with respect to that of the bundles.<sup>18,23</sup> To follow the evolution of  $Q_1$  and  $\beta$ , each XRD diagram is treated the same way: the derivative of the data in the neighborhood of the rising step is calculated and its local maximum is found by a fit (see the inset in Fig. 2).

#### IV. RESULTS AND DISCUSSION

The temperature evolution of  $Q_1$  and  $\beta$  is shown in Fig. 3, together with the thermal expansion coefficient  $\alpha(T) = \frac{1}{\langle L \rangle} \frac{\partial \langle L \rangle}{\partial T}$ , where  $\langle L \rangle = \frac{2\pi}{Q_1}$ . One should note here that this thermal expansion coefficient is different from the one shown

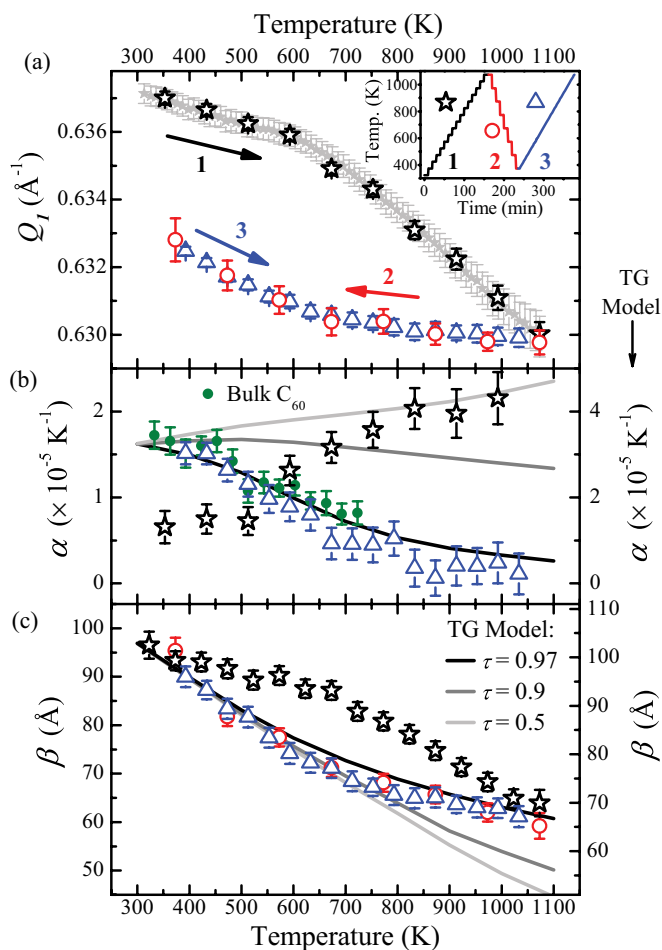


FIG. 3. (Color online) (a) Temperature evolution of the inflection point position  $Q_1$  measured following ramp 1 (empty stars, ID11 measurements; full gray stars, DIFFABS measurements) from 300 to 1073 K, as well as during ramps 2 and 3 (ID11 measurements). The inset shows the temperature cycle used for the measurements on ID11 as well as the correspondence of plotting symbols with the different ramps. (b) Thermal expansion coefficient  $\alpha(T)$  for ramps 1 (stars) and 2 and 3 (triangles), compared to that of reference bulk  $C_{60}$  (full circles) and to the ones calculated for filling rates of 0.5, 0.9, and 0.97 (lines). (c) Temperature evolution of the  $\beta$  parameter, compared to the one calculated for filling rates of 0.5, 0.9, and 0.97 (lines).

in Fig. 14 in Ref. 10, which corresponds to the calculated thermal expansion *inside one cluster*. Indeed, the  $Q_1$  value gives access to the mean interfullerene distance *in the whole chain*. We thus calculated, for comparison to experiment, a thermal expansion coefficient from the fit of the pair correlation function [Eq. (4) gives the mean interfullerene distance in the whole chain]. We will refer to the first ramp up, the ramp down, and the second ramp up as ramps 1, 2, and 3, respectively [inset to Fig. 3(a)]. During ramp 1 from room temperature up to 1073 K, both  $Q_1$  and  $\beta$  show a two-step decrease characterized by rather weak evolutions below  $\sim 650$  K (slopes of the curves), and a more pronounced decrease at higher temperatures. When cooling from 1073 to 350 K and heating again, the evolution of the parameters follows a different path: in contrast to what was observed for the first heating ramp, the temperature dependences of  $Q_1$  and  $\beta$  are increased below  $\sim 650$  K (larger

slopes of the curves). Both parameters superimpose for ramps 2 and 3. The value of  $Q_1$  at 350 K is smaller after ramp 2 than at the beginning of ramp 1, corresponding to a 0.6% expansion of the lattice parameter. This irreversibility shows that some relaxation processes have occurred during ramp 1.

Let us first discuss the *reversible* ramps 2 and 3. The experimental thermal expansion coefficient curve in Fig. 3(b) has a rounded step shape with  $\alpha$  evolving from  $1.7 \times 10^{-5} \text{ K}^{-1}$  at 350 K to about  $0.1 \times 10^{-5} \text{ K}^{-1}$  at high temperature. The higher calculated value of  $\alpha$  ( $3.2 \times 10^{-5} \text{ K}^{-1}$ ) indicates that the actual inter- $\text{C}_{60}$  potential is harder than the one used for the calculations.<sup>10</sup> Therefore, these calculations will be used as a guide to understand the data but do not allow fully quantitative comparisons. The initial value of  $\alpha$  is comparable to that of bulk  $\text{C}_{60}$  (Ref. 19) in its temperature range of stability. The high density of our peapods prevents any chain breaking, which reflects the similarity of the interaction potential between  $\text{C}_{60}$  molecules in these two systems. This behavior of a dense chain is well described by the TG model: in the calculated curves in Fig. 3(b), a similar evolution of  $\alpha$ , with a decrease below 600 K, is observed for very high filling rates—the best agreement between experiment and simulations being achieved for  $\tau = 0.97$ . For lower filling rates ( $\tau = 0.5$  or  $0.9$ ), the usual behavior of the thermal expansion observed for solid  $\text{C}_{60}$  (i.e., decreasing with  $T$ ) is competing with the formation of clusters in the chains—which tends to increase the average inter- $\text{C}_{60}$  distances. The result is a thermal expansion coefficient  $\alpha(T)$  that is constant (or increasing, for  $\tau \lesssim 0.7$ ) with temperature. The progressive vanishing of  $\alpha$  variation observed experimentally in our peapods at temperatures above 700 K—where bulk  $\text{C}_{60}$  no longer exists as a solid—can be attributed to the longitudinal confinement of the chains in the nanotubes: the chain expansion is restricted by the nanotube longitudinal expansion, which is very small [ $\alpha_{\text{SWNT}} \propto 5 \times 10^{-6} \text{ K}^{-1}$  at 1000 K (Ref. 20)].

The calculated  $\beta(T)$  curves are drawn in Fig. 3(c) for  $\tau = 0.5, 0.9$ , and  $0.97$ . They were simulated from Eq. (5), taking into account also the convolution with the experimental resolution function, which leads to smaller absolute values of  $\beta$ , as is illustrated in Fig. 1(b). The decrease of  $\beta$  with increasing temperatures corresponds to the increase of the root mean square deviation  $\sqrt{\sigma_1^2 + \sigma_2^2}$ —decrease of correlation length—and is a direct illustration of the increasing melting phenomenon predicted in Ref. 10. A good agreement with experiments, for ramps 2 and 3, is found for  $\tau = 0.97$ , with a

first rapid decrease followed by a slower one. This corroborates our previous conclusions, based on  $\alpha(T)$  behavior, of a very high effective filling rate of the studied peapods.

The data obtained during ramp 1 cannot be interpreted based on the same picture. Both the very low thermal expansion and weak  $\beta$  variation below 650 K suggest that an extra “pressure” is present inside the nanotubes,<sup>21</sup> making the chains more resilient to the melting. Above 650 K, the internal pressure is progressively released and thermal equilibrium is reached. Further experimental investigations are required to unambiguously determine the origin of this extra pressure, hypothesized as the origin of the nonreversible behavior reported here.

## V. CONCLUSION

A careful analysis of XRD data demonstrates the progressive melting occurring in a *dense* 1D chain of  $\text{C}_{60}$  molecules confined inside carbon nanotubes upon heating. It is characterized by a progressive increase of fluctuations in intermolecular distances, inducing a decrease of the slope of the sawtooth diffraction peak from fullerenes. This study of the *progressive* increase in cumulative fluctuations—characteristic of a 1D system—was only possible thanks to the exceptional temperature stability of the peapods, contrary to other known 1D systems.<sup>2–5</sup> The experimental data are well interpreted in light of the 1D Takashi-Gürsey model described in Ref. 10. Our results thus provide the experimental confirmation of theoretical predictions obtained in dense 1D systems. To achieve a full validation of these models, one would need to investigate the case of peapods with low filling rates (lower than 0.7). The observation of clustering in that case would translate in a constant or increasing  $\text{C}_{60}$  lattice thermal expansion with temperature.

## ACKNOWLEDGMENTS

The authors acknowledge H. Schober and H. Mutka (ILL) for stimulating discussion on the physics of fullerenes and on the problem of reduced dimensionality. Discussions with J. Cambedouzou (Laboratoire de Physique des Solides, Orsay and Institut de Chimie Séparative, Marcoule), on the physics of peapods and on their diffraction diagrams, were very useful. The authors also thank D. Thiaudière (synchrotron SOLEIL) and L. Hennet (UPR CNRS 3079, France) for helping in the use of the furnace at SOLEIL.

\*rols@ill.fr

†pascale.launois@u-psud.fr

<sup>1</sup>E. H. Lieb and D. C. Mattis, *Mathematical Physics in One Dimension: Exactly Soluble Models of Interacting Particles* (Academic Press, New York, 1966).

<sup>2</sup>I. U. Heilmann, J. D. Axe, J. M. Hastings, G. Shirane, A. J. Heeger, and A. G. MacDiarmid, *Phys. Rev. B* **20**, 751 (1979).

<sup>3</sup>E. Rosshirt, F. Frey, H. Boysen, and H. Jagodzinski, *Acta Crystallogr. Sect. B* **41**, 66 (1985).

<sup>4</sup>P. A. Albouy, J. P. Pouget, and H. Strzelecka, *Phys. Rev. B* **35**, 173 (1987).

<sup>5</sup>H. Grimm, H. Stiller, C. F. Majkrzak, A. Rupprecht, and U. Dahlborg, *Phys. Rev. Lett.* **59**, 1780 (1987).

<sup>6</sup>L. van Eijck, F. Merzel, S. Rols, J. Ollivier, V. T. Forsyth, and M. R. Johnson, *Phys. Rev. Lett.* **107**, 088102 (2011).

<sup>7</sup>B. Smith, M. Monthieux, and D. Luzzi, *Nature (London)* **396**, 323 (1998).

<sup>8</sup>S. Bandow, M. Takizawa, K. Hirahara, M. Yudasaka, and S. Iijima, *Chem. Phys. Lett.* **337**, 48 (2001).

- <sup>9</sup>M. Hodak and L. A. Girifalco, *Phys. Rev. B* **64**, 035407 (2001).
- <sup>10</sup>L. Girifalco and M. Hodak, *Appl. Phys. A* **76**, 487 (2003).
- <sup>11</sup>M. Hodak and L. A. Girifalco, *Phys. Rev. B* **68**, 085405 (2003).
- <sup>12</sup>B. Verberck, J. Cambedouzou, G. Vliegthart, G. Gompper, and P. Launois, *Carbon* **49**, 2007 (2011).
- <sup>13</sup>K. H. Michel, B. Verberck, and A. V. Nikolaev, *Phys. Rev. Lett.* **95**, 185506 (2005).
- <sup>14</sup>H. Kataura, Y. Maniwa, M. Abe, A. Fujiwara, T. Kodama, K. Kikuchi, H. Imahori, Y. Misaki, S. Suzuki, and Y. Achiba, *Appl. Phys. A* **74**, 349 (2002).
- <sup>15</sup>J. Cambedouzou, V. Pichot, S. Rols, P. Launois, P. Petit, R. Klement, H. Kataura, and R. Almairac, *Eur. Phys. J. B* **42**, 31 (2004).
- <sup>16</sup>R. C. Jones, *Acta Crystallogr.* **2**, 252 (1949).
- <sup>17</sup>H. Kataura, Y. Maniwa, T. Kodama, K. Kikuchi, K. Hirahara, and K. Suenaga, *Synth. Met.* **121**, 1195 (2001).
- <sup>18</sup>M. Chorro, J. Cambedouzou, A. Iwasiewicz-Wabnig, L. Noé, S. Rols, M. Monthieux, B. Sundqvist, and P. Launois, *Europhys. Lett.* **79**, 56003 (2007).
- <sup>19</sup>J. E. Fischer and P. A. Heiney, *J. Phys. Chem. Solids* **54**, 1725 (1993).
- <sup>20</sup>Y.-K. Kwon, S. Berber, and D. Tománek, *Phys. Rev. Lett.* **92**, 015901 (2004).
- <sup>21</sup>M. Yoon, S. Berber, and D. Tománek, *Phys. Rev. B* **71**, 155406 (2005).
- <sup>22</sup>Resolution width corresponds to crystalline chains ( $\sigma_1 = \sigma_2 = 0$ ) of  $\sim 500 \text{ \AA}$  long, i.e.,  $\sim 50$  molecules: chains with more than 50 molecules can be considered as infinite in our experiments.
- <sup>23</sup>Peapods form a 2D powder in the plane of the pellet and present a rather wide orientational distribution with respect to this plane (with a FWHM of  $\simeq 50^\circ$ ). The powder average performed in Eq. (5) can thus be used for data interpretation.